

See discussions, stats, and author profiles for this publication at: <https://www.researchgate.net/publication/231634596>

# Quantum Chemical Calculations on Novel Molecules from Xenon Insertion into Hydrocarbons

ARTICLE *in* THE JOURNAL OF PHYSICAL CHEMISTRY A · NOVEMBER 2002

Impact Factor: 2.69 · DOI: 10.1021/jp026777r

CITATIONS

62

READS

35

## 3 AUTHORS:



[Jan Lundell](#)

University of Jyväskylä

119 PUBLICATIONS 3,748 CITATIONS

SEE PROFILE



[Arik Cohen](#)

Hebrew University of Jerusalem

15 PUBLICATIONS 370 CITATIONS

SEE PROFILE



[Robert Benny Gerber](#)

University of California, Irvine

140 PUBLICATIONS 3,518 CITATIONS

SEE PROFILE

# Quantum Chemical Calculations on Novel Molecules from Xenon Insertion into Hydrocarbons

Jan Lundell,<sup>\*,†</sup> Arik Cohen,<sup>‡</sup> and R. Benny Gerber<sup>‡,§</sup>

Department of Chemistry, University of Helsinki, P.O. Box 55 (A. I. Virtasen aukio 1), FIN-00014 University of Helsinki, Finland, Department of Physical Chemistry, Hebrew University, Jerusalem 91904, Israel, and Department of Chemistry, University of California, Irvine, California 92697-2025

Received: August 16, 2002; In Final Form: October 16, 2002

Ab initio calculations have been performed on novel compounds that may greatly expand the scope of rare gas chemistry. These molecules are insertion compounds of xenon into unsaturated hydrocarbons, including acetylene, benzene, and phenol. We present computational evidence that molecules such as  $\text{H}-\text{Xe}-\text{C}_2\text{H}$ ,  $\text{H}-\text{Xe}-\text{C}_6\text{H}_5$ , and  $\text{H}-\text{Xe}-\text{OC}_6\text{H}_5$  exist. Computational results suggest also the existence of a series of xenon-insertion compounds for larger hydrocarbons of these types. The predictions are not restricted to molecules with only one xenon atom inserted in them but molecules such as  $\text{H}-\text{Xe}-\text{C}_2-\text{Xe}-\text{H}$  and  $\text{H}-\text{Xe}-\text{C}_2-\text{Xe}-\text{C}_2-\text{Xe}-\text{H}$  are computationally stable as well. This suggests the existence of linear polymers  $\text{H}-(\text{Xe}-\text{C}_2)_n-\text{Xe}-\text{H}$  for arbitrary large  $n$ . All predicted xenon-insertion molecules form a new class of possible precursors and intermediates for synthetic organic and organoelement chemistry.

## Introduction

The electronic structure of rare gas atoms in their ground state is extremely stable, causing the unique chemical inertness of these elements. Bartlett<sup>1,2</sup> prepared the first compound with a chemically bound xenon atom,  $\text{Xe}^+[\text{PtF}_6]^-$ . This was followed over the years by the preparation of a range of compounds of krypton, xenon, and radon.<sup>3–7</sup> In recent years, a renaissance in rare gas chemistry has taken place.<sup>8</sup> Especially, the use of fluorinated xenon compounds  $\text{XeF}_2$  and  $\text{XeF}_4$ , and their related cations  $[\text{XeF}]^+$  and  $[\text{XeF}_3]^+$  have had a dramatic effect on the advent of the chemistry of  $\text{Xe}-\text{C}$  compounds.<sup>9,10</sup> The  $[\text{FXe}^+]$  cation has been a basis for preparation of new xenon–carbon bonds due to its rather strong oxidation potential. Additionally, organoxenonium salts offer a promising access to new xenon–carbon compounds because they have lower oxidation potential than  $[\text{FXe}^+]$ . The stability and reactivity of organoxenonium salts  $[\text{RXe}][\text{Y}]$  depends on the nature of the organic group R and the counteranion  $[\text{Y}]^-$ .<sup>9</sup> The carbon bound to xenon in such a salt is also part of the aryl  $\pi$ -system. Here, the  $\text{Xe}-\text{C}$  bond is strengthened electrostatically because Xe polarizes the adjacent  $\pi$ -system, whereas an electron withdrawing fluorine substituent would make the aryl  $\pi$ -system electron-poor. Moreover, the more extended  $\pi$ -system tends to increase the stability of the  $\text{Xe}-\text{C}$  bond.<sup>9</sup>

Another major development in rare gas chemistry was the preparation and characterization of hydrides of the form  $\text{HRgY}$ , where Rg is a rare gas atom and Y is an electronegative group.<sup>11–15</sup> These compounds bear some similarity in electronic structure and nature of bonding to the organoxenonium salts because the stability of these compounds depend on the stability of the  $[\text{HRg}^+]$  cation and the electron affinity of Y. The  $\text{HRgY}$  molecules obtain their stability from ionic configurations and

they are best described as an ion pair  $\text{HRg}^+\text{Y}^-$ , even though they have a nonnegligible fraction of covalent character in the  $\text{Rg}-\text{Y}$  bond.<sup>16,17</sup> The  $\text{HRgY}$  molecules are strongly polar in their equilibrium structures, but experimental evidence in low-temperature matrixes indicates that they dissociate to their neutral fragments, i.e., via the  $\text{HRgY} \rightarrow \text{H} + \text{Rg} + \text{Y}$  dissociation channel.<sup>11,12,18</sup>

In this paper, a novel class of rare gas compounds is predicted that may greatly expand the scope of the field. The concepts of forming and stabilizing xenon-containing compounds in the way demonstrated for both organoxenonium salts and rare gas containing hydrides, have been elaborated further. Here, we characterize computationally several new insertion compounds of xenon into unsaturated hydrocarbons, including acetylene, benzene, and phenol. Thus: (1)  $\text{H}-\text{Xe}-\text{C}_2\text{H}$ ,  $\text{H}-\text{Xe}-\text{C}_6\text{H}_5$ , and  $\text{H}-\text{Xe}-\text{OC}_6\text{H}_5$  are shown to be computationally stable. This suggests also existence of a series of xenon inclusion compounds for larger hydrocarbons of these types. (2) Stability of  $\text{H}-\text{Xe}-\text{C}_2-\text{Xe}-\text{H}$  and  $\text{H}-\text{Xe}-\text{C}_2-\text{Xe}-\text{C}_2-\text{Xe}-\text{H}$  is predicted, suggesting existence of linear polymers  $\text{H}-(\text{Xe}-\text{C}_2)_n-\text{Xe}-\text{H}$  for arbitrary large  $n$ . The existence of these organoxenon hydrides seems to be a revolutionary new aspect of rare gas chemistry, as they differ completely from presently known compounds.

## Computational Methodology

The properties of the new compounds are studied by familiar ab initio methods, which by experience with other relevant compounds should be suitable here.<sup>11,12,19</sup> First a sufficiently high level of electronic structure theory is used to compute a minimum on the potential energy surface of the system that corresponds to the predicted molecule at its equilibrium structure. Electronic structure algorithms such as perturbation theory (MP2)<sup>20</sup> and coupled cluster (CCSD(T))<sup>20</sup> were employed for this purpose. For all xenon-containing compounds the averaged relativistic core potential by LaJohn<sup>21</sup> was used to describe xenon. The underlying d-shell was included in the valence yielding altogether 18 valence electrons, and the valence

\* Corresponding author. E-mail: jan.lundell@helsinki.fi.

<sup>†</sup> University of Helsinki.

<sup>‡</sup> Hebrew University.

<sup>§</sup> University of California.

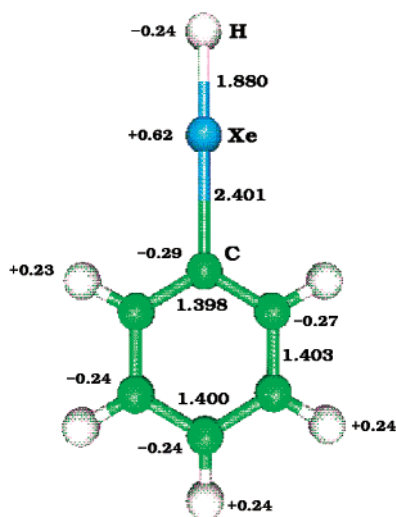


**Figure 1.** Equilibrium structure of  $\text{H-Xe-C}_6\text{H}_5$  computed at the MP2/LJ18/6-31+G(d,p) level. Interatomic distances (Å) are shown. Partial atomic charges (NBO) are indicated.

basis set was fully decontracted. This basis set is denoted as LJ18. For xenon-insertion compounds of benzene and phenol, the standard 6-31+G(d,p) basis set was used for economical reasons. For compounds derived from acetylene the larger 6-311++G(2d,2p) basis set was used to describe the H and C atoms.

The harmonic vibrational spectra of the compounds were computed from the electronic structure algorithms, to confirm that the stability is not marginal: High frequencies, i.e., stiff vibrations, indicate greater stability of the species. All the species studied here correspond to local, rather than global, minima on the potential energy surface: That is, the decomposition of  $\text{HRgY}$  into at least one set of products (e.g.,  $\text{HRgY} \rightarrow \text{Rg} + \text{HY}$  or  $\text{HRgY} \rightarrow \text{H} + \text{Rg} + \text{Y}$ ) is exoergic and is prevented from taking place only by the presence of energy barriers. Thus, the compounds are metastable, as are the Ar, Kr, and Xe hydrides reported.<sup>11–15</sup> Given a suitable preparation strategy, metastable compounds can be made, provided the protecting barriers are sufficiently high to prevent decay over the laboratory time scale. Energy differences between the species and relevant products are important properties, and were computed for the systems studied. Exploration of the full, multidimensional potential energy surface of the system is, of course, not feasible. For most systems, the potential surface was explored in the vicinity of the equilibrium structure, to provide some test of the existence of sufficiently high surrounding energy barriers. For several of the compounds, the potential energy along a coordinate leading from the local minimum to products was scanned, to assess the barrier along this transformation. In the present cases, essentially infinite tunneling decay times were estimated, predicting that the compounds are practically stable at temperatures close to 0 K.

## Results

**HXeC<sub>6</sub>H<sub>5</sub>: Xenon Inserted in Benzene.** The optimized equilibrium structure of planar  $\text{HXeC}_6\text{H}_5$  is shown in Figure 1. The computed Xe–H and Xe–C bond distances are 1.880 and 2.401 Å, respectively. The carbon–carbon bonds vicinal to the Xe–C bond appear only little affected by the Xe-insertion compared to the benzene monomer but the second C–C bonds are elongated from 1.398 to 1.403 Å, which indicate a slight stretch of the aryl ring. Similarly, the hydrogens attached to the carbon atoms are stretched out with increasing partial charge

of the carbon atoms. The C–H bond distances are predicted to be 1.087 Å for the C–H bond next to the Xe–C bonds, diminishing to 1.085 Å for the next C–H bonds, and being 1.084 Å for the C–H bond on the opposite side of the aryl ring from the Xe–C bond. The C–H bond distance computed for the benzene monomer at the MP2/6-31+G(d,p) level is 1.083 Å. The computed (NBO) partial charges of the various carbon-bound hydrogens are the same for all hydrogen atoms (+0.23). The computed atomic charge on Xe is +0.62, a negative charge of −0.29 resides on the carbon atom involved in the Xe–C bond, and the atomic charges within the  $\text{C}_6\text{H}_5$  ring are nonuniform: the negative partial charges on carbons diminish the further away the atom is from the positive Xe center. It must be noted that the hydrogen atom bound directly to Xe has a negative charge of −0.24, which is almost as large as those on the carbon atoms. This corresponds with the charge-transfer nature of the rare gas containing hydrides, in which also negatively charged hydrogens were found in the H–Xe tail.<sup>11,12</sup> Analysis of the bonding responsible for forming a H–Xe–Y functional group in the rare gas hydrides is partly ionic and partly covalent, the ionic contribution dominating in the Xe–Y bond and the covalent nature being prevalent in the Xe–H bond.<sup>16,17</sup> A similar nature of binding is found in  $\text{HXeC}_6\text{H}_5$  as well, with the exception that in this molecule the partial charge of the hydrogen bound to Xe is almost equal with the partial charge found on the atom attached to Xe from the electronegative moiety. In the  $\text{HRgY}$  molecules the atom of the attached moiety carries a larger negative partial charge than the hydrogen in the Xe–H group.<sup>11,12</sup>

The computed harmonic vibrational spectrum of  $\text{HXeC}_6\text{H}_5$  at the MP2/6-31+G(d,p) level is shown in Table 1. In general, the vibrational properties of this molecule are close to the benzene monomer computed at the same level of theory. The only significantly new vibrational absorptions are those due to the Xe–H tail of the molecule. The Xe–H stretching vibration is at 1317.7  $\text{cm}^{-1}$ , that of the Xe–C stretching mode is 178.3  $\text{cm}^{-1}$ . These are relatively stiff frequencies, corresponding to chemically bound molecules, rather than to weakly interacting van der Waals complexes. However, the estimated position of the Xe–H stretching is lower than typically found for this fingerprint vibration of the rare gas hydrides.<sup>11,12</sup> The strong ionic nature of the molecule, i.e.,  $[\text{HXe}^+][\text{C}_6\text{H}_5^-]$ , is highlighted in the computed infrared intensities. In accord with the rare gas hydrides, the Xe–H stretching is predicted to be very intense and the computed intensity is about 1500  $\text{km mol}^{-1}$ . The H–Xe–C bending mode at 985.3  $\text{cm}^{-1}$  is an intense vibrational mode and the predicted intensity is almost 190  $\text{km mol}^{-1}$ . On the contrary, the Xe–C stretching mode at 178.3  $\text{cm}^{-1}$  is predicted to be rather weak (9.6  $\text{km mol}^{-1}$ ). The two lowest frequencies at 114.7 and 92.4  $\text{cm}^{-1}$  are due to the bending and torsional vibrations of the H–Xe–C tail and these bands appear to be extremely weak.

The  $\text{HXeC}_6\text{H}_5$  molecule is predicted to be 5.47 eV higher in energy compared to the neutral fragment dissociation limit  $\text{Xe} + \text{C}_6\text{H}_6$ , but we estimate a high barrier along the H–Xe–C bending coordinate, which is sufficient to prevent the dissociation from taking place at low cryogenic temperatures. The metastable species is lower by 0.21 eV than the 3-body dissociation products  $\text{H} + \text{Xe} + \text{C}_6\text{H}_5$ , sufficient for stability against this process only at very low temperatures.  $\text{HXeC}_6\text{H}_5$  is related to the experimentally known  $\text{FXeC}_6\text{H}_5$ ,<sup>22</sup> but the hydrocarbon is expected to have many different properties from the fluorinated compound, e.g., as a starting reagent for further synthesis, where it should open many new possibilities. We

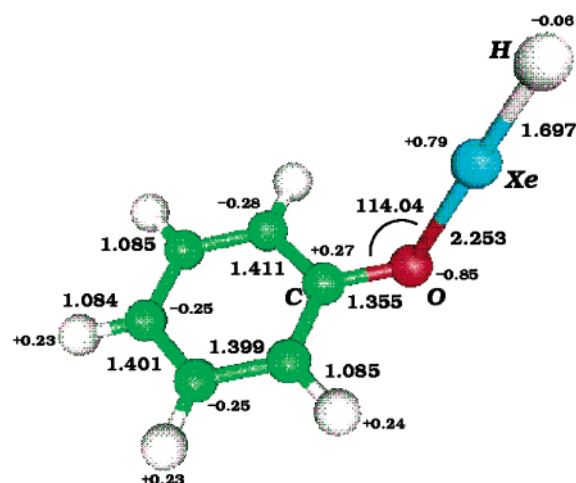


**Figure 2.** Equilibrium structure of H-Xe-OC<sub>6</sub>H<sub>5</sub> computed at the MP2/LJ18/6-31+G(d,p) level. Interatomic distances (Å) are shown. Partial atomic charges (NBO) are indicated.

**TABLE 1: MP2/LJ18/6-31+G(d,p) Computed Vibrational Frequencies (cm<sup>-1</sup>) and Infrared Intensities (km mol<sup>-1</sup>) for C<sub>6</sub>H<sub>5</sub>XeH and C<sub>6</sub>H<sub>5</sub>OxH**

	C <sub>6</sub> H <sub>5</sub> XeH		C <sub>6</sub> H <sub>5</sub> OxH	
	freq	IR intens	freq	IR intens
$\omega_1$	3267.3	31.8	3271.3	18.7
$\omega_2$	3248.5	35.9	3257.9	36.3
$\omega_3$	3241.4	2.9	3254.7	8.2
$\omega_4$	3213.1	20.9	3242.3	1.0
$\omega_5$	3212.3	0.0	3237.6	10.8
$\omega_6$	1639.4	0.0	1785.3	1741.9
$\omega_7$	1628.5	0.0	1652.3	302.6
$\omega_8$	1516.2	0.5	1635.9	2.9
$\omega_9$	1475.0	5.4	1529.5	305.5
$\omega_{10}$	1463.8	1.5	1498.5	0.0
$\omega_{11}$	1349.2	1.3	1447.0	1.2
$\omega_{12}$	1317.7	1500.7	1329.7	0.0
$\omega_{13}$	1219.5	0.0	1282.6	607.5
$\omega_{14}$	1198.5	0.0	1195.8	34.6
$\omega_{15}$	1102.3	3.0	1192.1	0.1
$\omega_{16}$	1079.1	2.9	1101.1	9.0
$\omega_{17}$	1027.6	1.6	1051.6	6.5
$\omega_{18}$	985.3	188.5	1012.7	0.9
$\omega_{19}$	896.5	0.0	894.9	0.8
$\omega_{20}$	878.2	0.1	884.7	0.3
$\omega_{21}$	860.5	0.3	846.0	10.9
$\omega_{22}$	833.8	0.0	843.4	67.9
$\omega_{23}$	709.4	70.9	812.5	0.3
$\omega_{24}$	626.0	15.4	734.0	78.4
$\omega_{25}$	620.7	1.3	659.7	2.3
$\omega_{26}$	609.9	63.6	625.0	0.2
$\omega_{27}$	600.7	28.9	610.9	3.4
$\omega_{28}$	386.1	0.3	550.3	18.9
$\omega_{29}$	367.2	0.0	528.7	7.9
$\omega_{30}$	340.0	0.0	443.1	1.1
$\omega_{31}$	178.3	9.6	408.0	3.9
$\omega_{32}$	114.7	0.2	397.4	0.1
$\omega_{33}$	92.4	0.7	367.1	85.1
$\omega_{34}$			188.2	13.9
$\omega_{35}$			60.4	3.4
$\omega_{36}$			19.4	3.1

speculate that a possible approach to synthesis may be based on the photochemistry of benzene in a low-temperature xenon matrix, in analogy to the preparation of the halogenated rare gas hydrides.<sup>11,12</sup>

**HXeOC<sub>6</sub>H<sub>5</sub>: Xe Inserted in Phenol.** The optimized equilibrium structure of HXeOC<sub>6</sub>H<sub>5</sub> at the MP2/6-31+G(d,p) level of theory is shown in Figure 2. Similarly to HXeC<sub>6</sub>H<sub>5</sub> and previously observed rare gas hydrides,<sup>11,12</sup> the insertion com-

pound follows the structural characteristics of the precursor molecule. For HXeOC<sub>6</sub>H<sub>5</sub> the O-Xe-H tail is bent out from the plane of the aryl ring and the computed bending angle is 114.0°. The Xe-H and Xe-O bonds are predicted to be shorter than the respective Xe-H and Xe-C bonds in HXeC<sub>6</sub>H<sub>5</sub>. The Xe-H bond distance of 1.697 Å is comparable with the value of 1.718 Å found for HXeOH at the MP2/LJ18/6-311++G-(2d,2p) level of theory.<sup>23</sup> It was found earlier that the MP2 computed estimates of the Xe-H bonds follow a general trend.<sup>12</sup> The Xe-H bond length decreases with increasing positive partial charge on xenon, which reflects the increasing ionic character of the molecule, indicating a more tightly bound species. HXeCN, which is the most strongly bound rare gas hydride known experimentally,<sup>23</sup> has a predicted Xe-H bond distance of 1.659 Å and a partial charge of +0.88 on Xe. For HXeOC<sub>6</sub>H<sub>5</sub> the value obtained for the Xe-H bond is very similar and the predicted partial charge on the Xe atom in this molecule is +0.79. The increased ionic nature is reflected in the computed vibrational frequency of the Xe-H bond. For HXeOC<sub>6</sub>H<sub>5</sub> this vibrational mode is predicted to lie at 1785.3 cm<sup>-1</sup> and it is a rather intense vibrational mode (1742 km mol<sup>-1</sup>).

The predicted Xe-O bond distance for HXeOC<sub>6</sub>H<sub>5</sub> is 2.253 Å, which correlates with the value of 2.208 Å found for HXeOH.<sup>23</sup> The O-Xe-H tail is found to be slightly tilted from linearity by less than 1°, whereas for HXeOH a tilt of almost 3° was noted.

The computed harmonic frequencies of HXeOC<sub>6</sub>H<sub>5</sub> are collected in Table 1, and the spectrum shows several intense bands along the Xe-H stretch. For example, the C-O stretch at 1282.6 cm<sup>-1</sup> and the Xe-O stretch at 367.1 cm<sup>-1</sup> could serve as possible fingerprint vibrations for this molecule in its experimental characterization.

The HXeOC<sub>6</sub>H<sub>5</sub> molecule is predicted to be 4.85 eV above that of the dissociated products Xe + C<sub>6</sub>H<sub>5</sub>OH. This metastable species is lower by only 0.07 eV than the 3-body dissociation products H + Xe + C<sub>6</sub>H<sub>5</sub>O. Even though the molecule appears at almost equal energy as its most likely dissociation limit, it must be remembered that metastable species can be experimentally made provided the protecting barriers are sufficiently high to prevent its decay. To obtain reliable estimates for these barriers is not trivial. In general, the potential energy surface near the equilibrium structure is described relatively well by modest theoretical methods like the perturbation theory used here. On the other hand, inclusion of highly sophisticated electron correlation methods is important when the potential energy surface is probed close to the dissociation limit. This is especially true when the HXeY molecule is stretched along the axis of the H-Xe tail-group. The adiabatic ionic surface responsible for the nature of the molecule in its equilibrium structure is crossed by a repulsive surface corresponding to the neutral fragments H + Xe + Y.<sup>25,26</sup> The dissociation limit of the HXeY molecules corresponds to that of the neutral fragments due to the avoided crossing between the neutral and ionic potential surfaces. Such a computational problem is inherently multiconfigurational in nature and is beyond our current study. The other dissociation channel leading to the global minimum via the bending of the H-Xe-O tail is more likely to be more single-configurational in nature, similar to the case of rare gas hydrides.<sup>11,12,25,26</sup> The potential energy surface was explored in some vicinity of the equilibrium structure, to provide some test of the existence of sufficiently high surrounding energy barriers. In the case of the HXeOC<sub>6</sub>H<sub>5</sub> molecule the H-Xe-O bending barrier appears to be high enough to stabilize the compound at experimental temperatures close to 0 K.



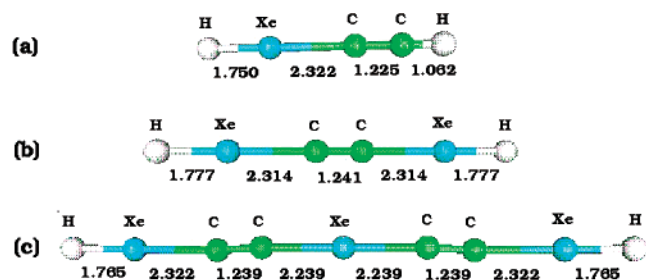


**Figure 3.** Equilibrium structure of (a)  $\text{H}-\text{Xe}-\text{C}_2-\text{H}$ , (b)  $\text{H}-\text{Xe}-\text{C}_2-\text{Xe}-\text{H}$ , and (c)  $\text{H}-\text{Xe}-\text{C}_2-\text{Xe}-\text{C}_2-\text{Xe}-\text{H}$  at the MP2/LJ18/6-311++G(2d,2p) level. Interatomic distances (Å) are shown. Note that the structure in (c) is slightly nonlinear, where the  $\text{C}-\text{C}-\text{Xe}$  angle is bent by ca.  $4^\circ$ .

**TABLE 2: MP2 and CCSD(T) Computed Harmonic Frequencies ( $\text{cm}^{-1}$ ) and Infrared Intensities ( $\text{km mol}^{-1}$ ) of HXeCCH**

assignment	MP2		CCSD(T) <sup>b</sup> freq
	freq	IR intens	
CH stretch	3462.3	30.7	3419.9
$\text{C}\equiv\text{C}$ stretch	1970.4	5.8	2000.4
$\text{Xe}-\text{H}$ stretch	1735.9	1515.3	1620.8
bend <sup>a</sup>	687.8	38.5	657.6
bend <sup>a</sup>	640.6	27.3	614.2
$\text{Xe}-\text{C}$ stretch	327.2	171.7	313.2
$\text{H}-\text{Xe}-\text{C}$ bend <sup>a</sup>	131.4	14.6	131.6

<sup>a</sup> Doubly degenerate. <sup>b</sup> The CCSD(T) optimized geometry is  $r(\text{Xe}-\text{H}) = 1.767 \text{ Å}$ ;  $r(\text{Xe}-\text{C}) = 2.351 \text{ Å}$ ;  $r(\text{C}\equiv\text{C}) = 1.223 \text{ Å}$ ;  $r(\text{C}-\text{H}) = 1.065 \text{ Å}$ .

**$\text{H}-\text{Xe}-\text{C}\equiv\text{CH}$ : Xenon Inserted in Acetylene.** The structure of this molecule is shown in Figure 3a. Both MP2 and CCSD(T) levels of theory were used to study this molecule, but rather small differences were found between the two levels for the optimized equilibrium structures. At the MP2 level the  $\text{Xe}-\text{H}$  bond distance is  $1.750 \text{ Å}$ , whereas the CCSD(T) calculation yields a slightly longer bond distance of  $1.767 \text{ Å}$ . Also for the  $\text{Xe}-\text{C}$  bond the CCSD(T) calculation gives a longer bond distance of  $2.351 \text{ Å}$  compared with  $2.322 \text{ Å}$  at the MP2 level. It is noteworthy, that both of these bonds are predicted to be shorter than in the experimentally observed HXeCN molecule, where the MP2/LJ18/6-311++G(2d,2p) values for  $\text{Xe}-\text{H}$  and  $\text{Xe}-\text{C}$  bonds are  $1.707$  and  $2.392 \text{ Å}$ , respectively.<sup>24</sup> This indicates that the HXeCCH molecule would be an even more stable structural configuration than the HXeCN molecule.

The computed harmonic frequencies of HXeCCH at both MP2 and CCSD(T) levels are collected in Table 2, and they predict qualitatively similar vibrational frequencies for various vibrational modes. At the MP2 level the  $\text{Xe}-\text{H}$  stretching frequency of HXeCCH is  $1735.9 \text{ cm}^{-1}$ , the  $\text{Xe}-\text{C}$  stretching frequency is  $327.2 \text{ cm}^{-1}$ , and both values fit the characteristics of a vibrationally stiff, chemically bound species. At the CCSD(T) level the  $\text{Xe}-\text{H}$  stretch is at  $1620.8 \text{ cm}^{-1}$ , which shows a rather typical shift compared with the MP2 result in accord with previous studies on rare gas hydrides.<sup>12,14,27</sup> In general, the large difference between the two electron correlation methods indicates a weakly bound system in line with, for example, HXeH<sup>25,28</sup> and HXeSH.<sup>29</sup> On the contrary, the high vibrational frequency of the  $\text{Xe}-\text{H}$  stretching mode suggests one of the most stable xenon-containing rare gas hydride discovered so far.<sup>11,12</sup> This assessment is supported by the high ionic degree of the  $\text{Xe}-\text{C}$  bond, whereas the  $\text{Xe}-\text{H}$  bond possesses a large covalent character. The NBO computed partial charge on Xe is  $+0.77$  and the H-atom bound to the Xe has a negative charge of  $-0.17$ . This leaves most of the negative partial charge on

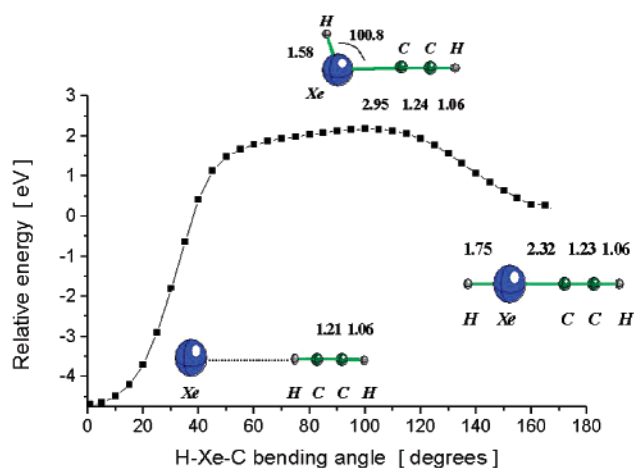


**Figure 4.** MP2/LJ18/6-311++G(2d,2p) potential energy of  $\text{H}-\text{Xe}-\text{C}_2-\text{H}$  along the  $\text{H}-\text{Xe}-\text{C}$  bending angle. The xenon compound corresponds to  $180^\circ$ ;  $\text{Xe} + \text{H}-\text{C}\equiv\text{C}-\text{H}$  corresponds to an angle of  $0^\circ$ . The transition state is at  $100.8^\circ$ .

the  $\text{C}_2\text{H}$  group. Interestingly, the carbon atom vicinal to the xenon is more negatively charged,  $-0.49$ , than the carbon bound to the hydrogen atom having a negative charge of  $-0.31$ . The hydrogen in the  $\text{C}_2\text{H}$  group has a partial charge of  $+0.20$ , and therefore, the charge distribution over  $\text{C}_2\text{H}$  appears nonuniform. The computed dipole moment for this species is  $2.66 \text{ D}$  at the MP2/LJ18/6-311++G(2d,2p) level.

The HXeCCH molecule is by  $1.46 \text{ eV}$  more stable than its three separate fragments  $\text{H} + \text{Xe} + \text{C}_2\text{H}$ . It is nevertheless a metastable species, with an energy of  $4.5 \text{ eV}$  above the energy limit of separated xenon and acetylene. Once formed, the metastable species is protected from decay by very high barriers: Figure 4 shows the computed (MP2) potential energy of the system versus the  $\text{H}-\text{Xe}-\text{C}$  bending angle (the molecular geometry at each angle was energy-optimized): There is a broad barrier of height of  $2.18 \text{ eV}$  along the  $\text{H}-\text{Xe}-\text{C}$  bending coordinate for the process  $\text{H}-\text{Xe}-\text{C}_2\text{H} \rightarrow \text{Xe} + \text{C}_2\text{H}_2$ . With such a barrier, decay by tunneling is totally negligible even for temperatures well above the cryogenic range.

**$\text{H}-\text{Xe}-\text{C}_2-\text{Xe}-\text{H}$  and  $\text{H}-\text{Xe}-\text{C}_2-\text{Xe}-\text{C}_2-\text{Xe}-\text{H}$ : Toward Xenon-Acetylene Polymers.** The equilibrium geometries of the two species are shown in Figures 3a and 3b, respectively. These predicted compounds seem very different in constitution and in many properties from the presently known rare gas compounds.  $\text{H}-\text{Xe}-\text{C}_2-\text{Xe}-\text{H}$  is a linear and centrosymmetric species. The predicted  $\text{Xe}-\text{H}$  bond distance is  $0.027 \text{ Å}$  longer and the  $\text{Xe}-\text{C}$  bond distance  $0.008 \text{ Å}$  shorter than in the HXeCCH molecule. Also, the  $\text{C}-\text{C}$  bond distance is  $0.016 \text{ Å}$  longer in  $\text{HXeC}_2\text{XeH}$  than in HXeCCH. There is also a pattern of charge alterations: the H atoms have partial charges of  $-0.20$ , the Xe atoms have charges of  $+0.75$ , and both of the carbon atoms bear a negative charge of  $-0.55$ . Inserting a second xenon atom into HXeCCH decreases the positive charge on xenon and increases the negative charge of the hydrogen in the other  $\text{Xe}-\text{H}$  end of the molecule.

Explorations of energy for configurations away from equilibrium suggest relative high barriers for decomposition of this species. The stability of this molecule against its three-body dissociation channel ( $\text{HXeC}_2\text{XeH} \rightarrow \text{H} + \text{Xe} + \text{C}_2\text{XeH}$ ) can be thought to rely heavily on the stability of an exotic  $\text{C}_2\text{XeH}$  radical product in analogy with the experimentally characterized HXeNCO,<sup>30</sup> HXeCN,<sup>24</sup> HXeSH,<sup>29</sup> or HXeOH<sup>23</sup> molecules. However, computations show that this radical species is stable and that the  $\text{H} + \text{Xe} + \text{C}_2\text{XeH}$  dissociation limit is almost

**TABLE 3: MP2/LJ18/6-311++G(2d,2p) Computed Vibrational Frequencies ( $\text{cm}^{-1}$ ) and Infrared Intensities ( $\text{km mol}^{-1}$ ) of  $\text{HXeC}_2\text{XeH}$  and  $\text{HXeC}_2\text{XeC}_2\text{XeH}$** 

$\text{HXeCCXeH}$			$\text{HXeC}_2\text{XeC}_2\text{XeH}$	
approx assignment	freq	IR intens	freq	IR intens
$\nu(\text{C}\equiv\text{C})$	1967.9	0.0	1979.6	16.0
$\nu_s(\text{Xe}-\text{H})$	1670.8	0.0	1977.6	0.0
$\nu_{as}(\text{Xe}-\text{H})$	1594.7	5450.5	1679.6	0.2
$\delta(\text{H}-\text{Xe}-\text{C})$	667.1 <sup>a</sup>	47.5	1655.9	6353.2
$\delta(\text{H}-\text{Xe}-\text{C})$	651.6 <sup>a</sup>	0.0	663.4	37.6
$\nu_{as}(\text{Xe}-\text{C})$	454.2	735.3	663.2	0.5
$\delta(\text{XeC}\equiv\text{CXe})$	129.7	0.0	661.8	11.4
$\nu_s(\text{Xe}-\text{C})$	60.3 <sup>a</sup>	11.0	661.8	26.7
$\delta(\text{XeC}\equiv\text{CXe})$	48.1 <sup>a</sup>	0.0	483.2	0.0
			447.4	2020.7
			281.2	18.3
			253.6	22.0
			179.9	0.0
			155.9	0.0
			149.9	0.0
			102.7	6.9
			82.2	6.7
			60.2	0.0
			59.4	0.0
			50.5	10.5
			12.5	1.1

<sup>a</sup> Doubly degenerate.

2.7 eV above the  $\text{HXeC}_2\text{XeH}$  molecule.<sup>31</sup> This indicates good prospects to produce and characterize this molecule experimentally, which would make it the first neutral rare gas hydride containing two xenon atoms in it. Even then, this molecule is still a metastable species, being 9.3 eV above the global energy minimum  $2\text{Xe} + \text{HCCH}$  and about 6.5 eV above the  $2\text{Xe} + \text{H}_2 + \text{C}_2$  dissociation limit.

The computed harmonic vibrational spectrum of  $\text{HXeC}_2\text{XeH}$  is presented in Table 3. The vibrational frequencies for a molecule of this size are relatively high. There are two Xe–H stretching modes: the symmetric, infrared inactive band is at  $1670.8\text{ cm}^{-1}$ , and the intense ( $5450.5\text{ km mol}^{-1}$ ) antisymmetric Xe–H stretch is predicted to lie at  $1594.7\text{ cm}^{-1}$ . Compared with previously characterized rare gas hydrides, the position of the computed Xe–H stretching frequency indicates a medium bound compound with a Xe–H stretching frequency between those of  $\text{HXeSH}$  ( $1523.1\text{ cm}^{-1}$ ) and  $\text{HXeBr}$  ( $1684.5\text{ cm}^{-1}$ ). The intense antisymmetric Xe–C stretch is found at  $454.2\text{ cm}^{-1}$ , but the symmetric stretch is found as low in the spectrum as  $60.3\text{ cm}^{-1}$ .

The prediction of a linear, size-scalable polymer with multiple rare gas atoms seems to us particularly interesting and chemically new in the area of noble gas chemistry. The structure of  $\text{H}-\text{Xe}-\text{C}_2-\text{Xe}-\text{C}_2-\text{Xe}-\text{H}$  is slightly bent: The C–C bond forms an angle of  $\sim 4^\circ$  with the axis of the neighboring Xe–H. The energy difference between the equilibrium structure and a complete linear structure is only  $0.02\text{ kJ mol}^{-1}$  ( $2.07 \times 10^{-4}\text{ eV}$ ), which indicates that, vibrationally averaged, this molecule appears as a linear species. It is remarkable that in all acetylene-derived Xe compounds the Xe–H tailgroup of the molecule appears to be similar. The MP2-computed bond distances in all these molecules are about  $1.76\text{ \AA}$ , and the partial charges of the xenon and hydrogen are about  $+0.77$  and  $-0.20$ , respectively. Therefore, the Xe–H tail of the molecule is quite insensitive to the changes in the central part of the molecule. By computed frequencies shown in Table 3, and by exploration of configurations away from equilibrium, all these species appear rather stable. Qualitatively, there seems to be no drastic decrease in relative stability among these compounds. In fact, we find

very small differences of bond distances and vibrational frequencies in the characteristic Xe–H group of these molecules, even though this group is very sensitive toward the changing stability of the species.<sup>11,12</sup> Calculations for higher polymers of this family at a reliable level are becoming computationally too demanding, but on the basis of the above findings, it seems reasonable to extrapolate that polymers of arbitrary size  $\text{H}-(\text{XeC}_2)_n-\text{XeH}$  could be stable. Indeed, if their stability should keep above the cryogenic regime, they would provide a very novel type of rare gas compound.

## Conclusions

Ab initio calculations have been performed on novel insertion compounds of xenon into unsaturated hydrocarbons. Computational evidence shows that molecules such as  $\text{HXeC}_2\text{H}$ ,  $\text{HXeC}_6\text{H}_5$ , and  $\text{HXeOC}_6\text{H}_5$  exist. These molecules suggest a new class of compounds that widen the scope of the field of Xe–C chemistry. Predictions were also made on acetylene derivatives containing more than one xenon atom, which suggest that polymers of  $\text{H}-(\text{XeC}_2)_n-\text{XeH}$  with an increasing number of  $n$  could be stable. All predicted molecules are metastable compared to their global minima, but in analogy with the recently discovered rare gas hydrides, this does not exclude their possible existence. On the contrary, they appear as possible gateways to novel high energy materials. Given a suitable preparation strategy, sufficiently high protecting barriers can prevent their decay over laboratory time scales. The similarity of these molecules to the rare gas hydrides suggests that their most probable dissociation channel is the 3-body channel producing a hydrogen atom, a xenon atom, and a hydrocarbon radical. Surprisingly, computations on the energy differences between species show that all predicted molecules are of lower energy than their separate fragments. All in all, the hydrocarbon compounds are potential precursors for novel xenon-containing compounds. The sufficient stability of these Xe–C compounds could open up a new direction for future investigations that could have an impact on the chemistry of novel Xe–C compounds finding their usefulness in synthetic organic and organoelement chemistry. Especially, the computed stability of the  $\text{HXeCCCH}$  molecule suggests that this species should be a very likely candidate for experimental detection. Its predicted stability in analogy with experimentally observed rare gas hydrides should warrant preparation of this molecule at least by matrix photochemistry in analogy to the rare gas hydrides.

**Acknowledgment.** We thank Profs. J. Nowick and D. Van Vranken for discussions and Z. Bihary for critical comments on the manuscript. J.L. thanks the Finnish Cultural Foundation and the Academy of Finland for financial support. R.B.G. thanks the Chemistry Division of NSF for support of the work at UC Irvine (Grant CHE-0101199). Work at the Hebrew University was supported by the DFG Germany (project Sfb 450). CSC-Center for Scientific Computing Ltd. (Espoo, Finland) is thanked for allocated computer time.

## References and Notes

- (1) Bartlett, N. *Proc. Chem. Soc.* **1982**, 218.
- (2) Graham, L.; Graudejus, O.; Jha, N. K.; Bartlett, N. *Coord. Chem. Rev.* **2000**, 197, 321.
- (3) Nelson, L. Y.; Pimentel, G. C. *Inorg. Chem.* **1967**, 6, 1758.
- (4) Turner, J. J.; Pimentel, G. C. *Science* **1963**, 140, 974.
- (5) Holloway, J. H.; Hope, E. G. *Adv. Inorg. Chem.* **1999**, 46, 51.
- (6) Grills, D. C.; George, M. W. *Adv. Inorg. Chem.* **2001**, 52, 113.
- (7) Stein, L. *Nature* **1973**, 243, 30.

- (8) Christe, K. O. *Angew. Chem., Int. Ed.* **2001**, *40*, 1419.
- (9) Frohn, H.-J.; Bardin, J. J. *Organometallics* **2001**, *20*, 4750 and references therein.
- (10) Brel, V. K.; Pirkuliev, N. Sh.; Zefirov, N. S. *Russ. Chem. Rev.* **2001**, *70*, 231.
- (11) Pettersson, M.; Lundell, J.; Räsänen, M. *Eur. J. Inorg. Chem.* **1999**, 729.
- (12) Lundell, J.; Khriachtchev, L.; Pettersson, M.; Räsänen, M. *Low Temp. Phys.* **2000**, *26*, 680.
- (13) Khriachtchev, L.; Pettersson, M.; Runeberg, N.; Lundell, J.; Räsänen, M. *Nature* **2000**, *406*, 874.
- (14) Lundell, J.; Chaban, G. M.; Gerber, R. B. *Chem. Phys. Lett.* **2000**, *331*, 308.
- (15) Wong, M. W. *J. Am. Chem. Soc.* **2000**, *112*, 6289.
- (16) Berski, S.; Latajka, Z.; Silvi, B.; Lundell, J. *J. Chem. Phys.* **2000**, *114*, 4349.
- (17) Berski, S.; Silvi, B.; Lundell, J.; Noury, S.; Latajka, Z. In *New Trends in Quantum Chemistry and Physics*; Maruani, J., Minot, C., McWeeny, R., Smeyes, Y. G., Wilson, S., Eds.; Kluwer: Dordrecht, 2001; Vol. 1, pp 259–279.
- (18) Pettersson, M.; Nieminen, J.; Khriachtchev, L.; Räsänen, M. *J. Chem. Phys.* **1997**, *107*, 8423.
- (19) Lundell, J.; Pettersson, M.; Räsänen, M. *Comput. Chem.* **2000**, *24*, 325.
- (20) Jensen, J. *Introduction to Computational Chemistry*; Wiley: Chichester, U.K., 1999.
- (21) LaJohn, L. A.; Christiansen, P. A.; Ross, R. B.; Atashroo, T.; Ermler, W. C. *J. Chem. Phys.* **1987**, *87*, 2812.
- (22) Frohn, H.-J.; Thiessen, M. *Angew. Chem., Int. Ed.* **2000**, *39*, 4591.
- (23) Pettersson, M.; Khriachtchev, L.; Lundell, J.; Räsänen, M. *J. Am. Chem. Soc.* **1999**, *121*, 11904.
- (24) Pettersson, M.; Lundell, J.; Khriachtchev, L.; Räsänen, M. *J. Chem. Phys.* **1998**, *109*, 618.
- (25) Runeberg, N.; Seth, M.; Pyykkö, P. *Chem. Phys. Lett.* **1995**, *246*, 239.
- (26) Runeberg, N.; Pettersson, M.; Khriachtchev, L.; Lundell, J.; Räsänen, M. *J. Chem. Phys.* **2001**, *114*, 836.
- (27) Lundell, J.; Chaban, G. M.; Gerber, R. B. *J. Phys. Chem. A* **2000**, *104*, 7944.
- (28) Pettersson, M.; Lundell, J.; Räsänen, M. *J. Chem. Phys.* **1995**, *103*, 205.
- (29) Pettersson, M.; Lundell, J.; Khriachtchev, L.; Isoniemi, E.; Räsänen, M. *J. Am. Chem. Soc.* **1998**, *120*, 7979.
- (30) Pettersson, M.; Khriachtchev, L.; Lundell, J.; Jolkkonen, S.; Räsänen, M. *J. Phys. Chem. A* **2000**, *104*, 3579.
- (31) At the MP2/LJ18/6-311++G(2d,2p) level the CCXeH radical is linear with bond distances of  $r(\text{Xe}-\text{H}) = 1.639 \text{ \AA}$ ,  $r(\text{C}-\text{Xe}) = 2.352 \text{ \AA}$ , and  $r(\text{C}-\text{C}) = 1.884 \text{ \AA}$ .